Available online at www.sciencedirect.com

ScienceDirect

Procedia Engineering 160 (2016) 262 – 269

Procedia Engineering

www.elsevier.com/locate/procedia

XVIII International Colloquium on Mechanical Fatigue of Metals (ICMFM XVIII)

Mixed mode (I+II) fatigue crack growth of long term operating bridge steel

G. Lesiuk[a, *], P.Kucharski[a], J.A.F.O. Correia[b], A.M.P. De Jesus[b], C. Rebelo[c], L. Simões da Silva[c]

[a] *Faculty of Mechanical Engineering, Department of Mechanics, Material Science and Engineering, Wrocław University of Science and Technology, Smoluchowskiego 25, 50-370 Wrocław, Poland.*
[b]*INEGI/Faculty of Engineering, University of Porto, Rua Dr. Roberto Frias, 4200-465 Porto, Portugal.*
[c] *ISISE/Department of Civil Engineering, University of Coimbra, Rua Luís Reis Santos, Pólo II, 3030-788 Coimbra, Portugal.*

Abstract

The structural components from structures such as bridge members are subjected to a long operating period of time. The problem of fatigue cracks is more interesting in existing bridge structures with existing cracks. In case of the structures erected at the turn of the 19th and 20th centuries, the cracks are natural elements of the old steel metallic structures. The uniaxial fatigue crack growth description lead us often to significant errors in predicting of a residual lifetime. As a good example, it can be a residual lifetime of the riveted joints in such a type of structures. On the other hand, the 19th century structures were erected with puddled iron or low carbon mild rimmed steel. The experimental results [1,2] obtained by authors, have shown that the fatigue cracks grow much faster than its modern equivalent. This phenomenon is supported by microstructural degradation processes [2]. In this paper some examples of degenerated microstructures have been presented. In order to fill a lack in experimental data in the literature, the results of a mixed mode (I+II) fatigue crack growth have been presented and discussed within the background of Fracture Mechanics models. All the results have been implemented into the Abaqus environment.

Peer-review under responsibility of the University of Oviedo

Keywords: Mixed-mode loading; fatigue crack growth; puddled steel; bridges.

* Corresponding author. Tel.: +48 71 320 39 19; fax: +48 71 321 12 35.
E-mail address: grzegorz.lesiuk@pwr.edu.pl

1877-7058
Peer-review under responsibility of the University of Oviedo
doi:10.1016/j.proeng.2016.08.889

1. Introduction

The maintenance of the long-term operated structures, such as bridges, plays an important role in transportation safety. The high hazard factor seems to be the oldest structures. Therefore a special attention should be paid for the structures erected at the turn of the 19th and 20th centuries. Till today, the significant part of those bridges (older than 100. years) are still operating. It was estimated that in Poland, in the 70s, more than 10% of bridges constructed using puddled steel were still in operation (based on Madaj [3]). According to Suresh [4], about 40% in weight of the metallic railway bridges currently in service in France are puddled iron hot riveted structures. From the safety point of view the essential knowledge is the estimation of the pre-critical fatigue crack growth. The works [5, 6] and recommendations [7, 8] underline the role of Fracture Mechanics in the safety level evaluation. On the other hand, almost all works propose only the recommendations and collect experimental data for pure mode I loading condition. It is observed – especially in puddle iron – that numerous non-metallic inclusions and their random distribution lead to the local mixed mode loading state ahead of the crack tip (or large nonmetallic inclusions). It is also observed that the brittleness of these long term operated "archaic" type of steel show tendency to the microstructural degradation processes [2]. These processes support the brittleness of the material. However, in mixed mode loading it seems that nonmetallic inclusions have the major influence in the propagation behaviour. . This paper is an attempt in filling the lack in literature with the experimental data of fatigue crack growth rate and analysis of crack paths in long term operated structural component made from puddle iron under mixed-mode condition.

In mixed mode fatigue crack propagation an important part of investigation is, not only the description of the fatigue crack growth rate but also the analysis of the crack paths – the angular direction (crack branching) of fatigue crack growth (θ). The most widely used criteria for mixed mode fatigue crack propagation are: maximum energy release rate (MERR), [9] the maximum tangential stress (MTS), [10] and strain energy density (SED), [11, 12]. The MTS criterion assumes that the direction of crack growth is connected with the direction, where the tangential stress reaches its maximum value. For the unification of the results comparison in terms of mixed mode (I+II) loading, the elastic-mixity parameter M_e has been defined as:

$$M_e = \frac{2}{\pi} a\tan\left(\frac{K_I}{K_{II}}\right). \quad (1)$$

The value M_e=0 corresponds with pure shear state (mode II) and the value M_e=1 means that the specimen is loaded in pure mode I. According to [10], for the MTS criterion, crack growth direction satisfy the following equation:

$$K_I \sin(\theta) + K_{II}(3\cos(\theta) - 1) = 0. \quad (2)$$

In case of the SED criterion, the main assumption consist in the hypothesis that the crack stable propagation occurs in the direction along which the strain energy density factor S, reaches a minimum value. The unstable propagation/ final fracture occurs when this factor reaches a critical value S_c [11, 12].

2. Material investigation of the delivered puddle iron member

Two steel members (dated from 1863) were obtained for the investigation from the restored viaduct in Brochocin (Low Silesia, Poland). In order to identify the type of old metallic material (puddle steel or old mild steel), the chemical composition was evaluated by means of gravimetric method and spectroscopy. The results of analysis (0.08%C, 0.025%Mn, 0.15%Si, 0.245%P, 0.015%S) seem to confirm that the investigated material is a puddle iron. The microstructure of tested material is shown in Fig. 1. The static tensile test results confirmed the brittle nature of this old metallic material (YTS=286.5 MPa, UTS=359.7MPa, E=191GPa, elongation at break A=15.3%, necking Z=33.9%). Due to the material limitation and thickness of the member (t=7mm) with corrosion pits, Charpy impact tests were not performed. This type of test in many cases could be treated as a tool to evaluate the microstructural degradation of the material in terms of the comparison of results in post operated and normalized state. Therefore, the influence of the microstructural degradation processes is not a major topic in this paper. In most cases, the rapidly decreasing impact energy in post operated state was caused by the microstructural degradation – two examples are described in another paper [2].

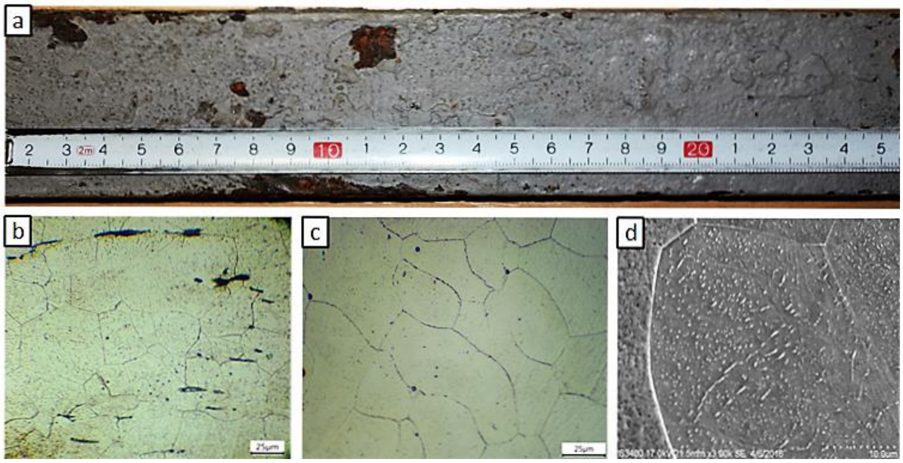

Fig. 1. Material delivered for the investigation; (a) general view of the member (L=1m); (b) ferrite grains structure with the nonmetallic inclusions and numerous separations of the brittle phases inside ferrite grans – post-operated state, etched 3%HNO_3, light microscopy; (c) specimen after normalization (950°, 2h, air) − remaining brittle phases inside ferrite grains, etched 3%HNO_3, light microscopy; (d) enlarged grain of ferrite with thick envelope of the Fe_3C_{III} on the grain boundary with the numerous of brittle separations inside ferrite grains, post-operated state, etched 3%HNO_3, SEM.

3. Mixed mode (I+II) fatigue crack growth in puddle iron

The pure mode I fatigue crack growth results were presented in [13]. In order to obtain the kinetic fatigue fracture diagrams in terms of mixed mode loading conditions, the experimental measurements were arranged in accordance to the Richard conception [14]. For the mixed mode loading condition performance, the CTS (compact tension shear specimen) were used. Due to the material limitations, the main dimensions were equal: W=42 mm, t=6.8mm. The initial notch with precrack (mode I condition) satisfied the CTS – Richard [14] suggestions for the normalized crack length a/W=0.52÷0.55. The additional fixtures for CTS specimen and measurement setup is shown in Fig. 2.

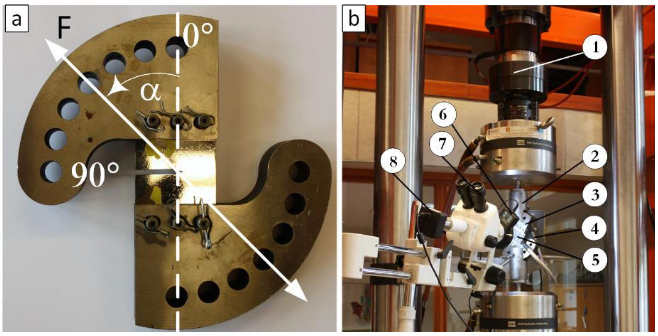

Fig. 2. Measurement setup and specimen during test; (a) equipment – CTS specimen fixture for uniaxial testing machine, (b) experimental setup; 1 – 50kN MTS load cell, 2 – clevis, 3 – CTS specimen holder, 4 – light source 1, 5 – CTS specimen, 6 – led light source, 7 – eyepieces, 8 – digital CMOS camera integrated with the measurement system operated by the PC and FlexTest console.

Initial U-notch was performed by electro-discharging machining (EDM, ρ<0.3mm). The specimens were grinded and polished to a mirror surface in order to increase the possibilities of the successful optical observation of fatigue crack. All specimens were precracked under mode I condition, with the same procedure; the initial load was 6kN (R=0.1) and after 125000 cycles the load has been decreased to the level 4.5 kN (R=0.1). After reaching, the total number of cycles equal to 200000 the specimens were loaded with the desired mixed mode loading condition (30 and 45 degrees). During the experiments, the constant force amplitude was involved. The maximum value of load was kept on the level 6500N (R=0.1) with the frequency of 10Hz. The crack length was monitored with the travelling microscope. The high-resolution CMOS (15Mp) camera cyclically recorded the images (with the resolution 65pix/mm). The crack length was measured in x and y directions. The virtual origin of the coordinate system has been localized at the end of the pre crack. The x-axis was oriented along the notch. After the experiments, the crack lengths were calculated by the correlation of the periodically registered pairs of the (x,y) crack tip coordinates. In order to obtain the kinetic fatigue fracture diagram, the stress intensity factor values for each pair of the coordinates were computed.

3.1. Numerical estimation of the stress intensity factors

The initial stress intensity factors has been obtained using a close-form solution, proposed by Richard [14]:

$$K_I = \frac{\Delta F\sqrt{\pi a}\cos(\alpha)}{Wt(1-a/W)}\sqrt{\frac{0.26+2.65(a/W-a)}{1+0.55(a/W-a)-0.08(a/W-a)^2}}, \tag{3}$$

$$K_{II} = \frac{\Delta F\sqrt{\pi a}\sin(\alpha)}{Wt(1-a/W)}\sqrt{\frac{-0.23+1.4(a/W-a)}{1-0.67(a/W-a)+2.08(a/W-a)^2}}, \tag{4}$$

where: ΔF – applied load range, a – crack length, W – specimen width, t – specimen thickness and α describes the loading angle – defined in Fig. 2a. The equations (3-4) are valid in range 0.5≤a/W≤0.7. However, the mentioned SIF-formulas are valid only for slant cracks. During the experiments the crack curvature has been observed. In global view, it can be treated as kinked crack with the kinking angle θ. After the experiments, all results of the crack tip coordinate pairs were estimated by a straight line (for all cases $R^2>0.95$). In order to obtain the actual values of the stress intensity factors K_I, K_{II}, the numerical procedure has been involved. All simulations were performed in Abaqus 6.14 environment . In order to estimate stress intensity factors, linear Fracture Mechanics was assumed, which resulting linear material model. Richard's specimen geometry and boundary conditions was presented in Figure 3. Two different kinds of constraints were considered regarding the works by Borrego [15] and Zafosnik [16]. Finally, the first method was rejected, due to imposing artificial stress, which has an impact on stress intensity factors, as well as crack propagation direction. Fatigue crack was modeled as a stationary one, with constant increments equal to 0.5 mm. Crack paths were obtained during the experiment, and the assumption, that crack is strictly straight line was made. For 30° loading case, crack was propagated at the angle of 50°, and for 45° loading case at the angle 64°, respectively. Initial crack was equal to 20.8 mm with additional 1.2 mm precracking. Loading were transmitted through rigid pins, and the maximum output force F with the value of 6.5 kN was decomposed in the following components:

$$F_1 = F(0.5\cos\alpha + (c/b)\sin\alpha), \tag{5}$$

$$F_2 = F\sin\alpha, \tag{6}$$

$$F_3 = F(0.5\cos\alpha - (c/b)\sin\alpha), \tag{7}$$

where c and b are equal to 25.2 mm. Moreover, in computations plane strain conditions were assumed.

Stress intensity factors were obtained using quarter point elements and the J-integral method. Quadratic plane stress elements with reduced integration (CPE8R) and mid – side nodes moved by 0.25 times the side length where used at crack tip to capture stress singularity at crack tip $\frac{1}{\sqrt{r}}$ singularity. In the remaining region, triangular and rectangular second – order elements were used. Total number of elements varies between iterations (crack increments), however the approximate amount of elements was in the order of 2500.

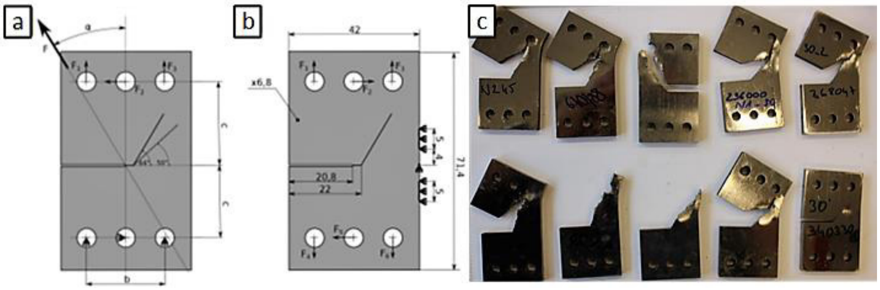

Fig. 3. CTS specimen main dimensions and considered boundary conditions; (a) specimen geometry, (b) artificial constraints at the edge of specimen, (c) broken specimens after tests.

The mesh pattern is shown in Fig. 4. Stress intensity factors (K_I, K_{II}) were obtained for different crack lengths. The maximum tangential stress criterion was used to establish the equivalent stress intensity factor, which was used to compute the fatigue live curves which were compared with the experimental results. The equivalent Huber-Mises stress distribution is shown in Fig. 5.

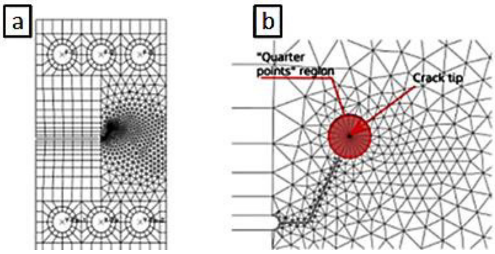

Fig. 4. Mesh pattern in CTS simulation; (a) overall mesh; (b) element configuration at the crack tip vicinity.

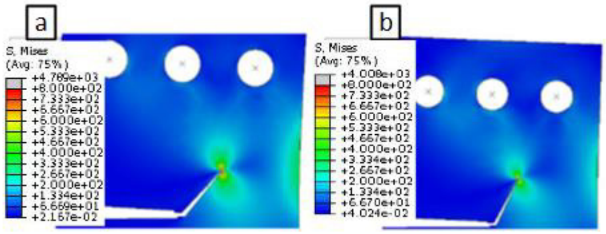

Fig. 5. Huber-Mises stress distribution in CTS specimen for: (a) 30° loading case; (b) 45° loading case.

3.2. Experimental results

Fatigue crack growth curves is shown in Fig. 6 for all specimens. The fatigue crack growth rate has been successfully obtained using the combined secant method and partially differentiation of the fatigue crack curve (using polynomial or exponential function – in case of the fitting R^2>0.93).

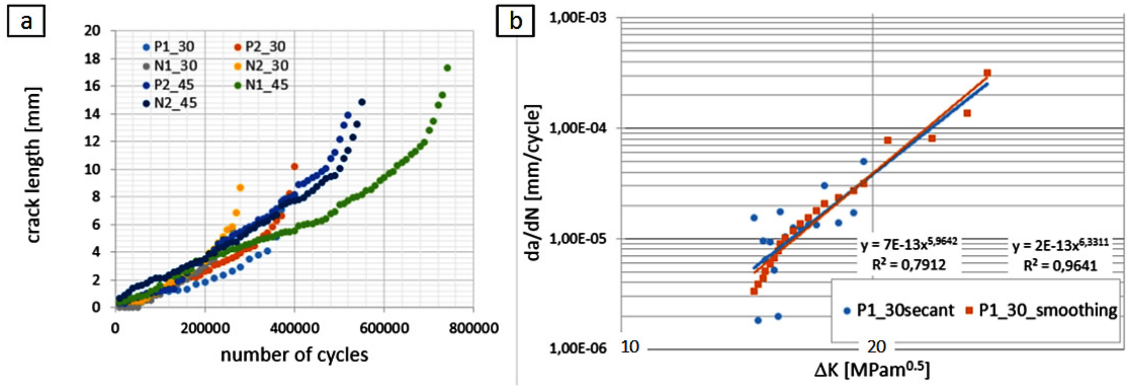

Fig. 6. (a) Fatigue crack length vs. number of cycles for all tested specimens; (b) FCGR curves comparison before (direct secant method) and after the smoothing process (combined exponential differentiation and secant method) for P1_30 specimen in terms of ΔK_{eq}.

For all specimens, the exponential model do not satisfactorily described the data, the non-exponential parts being solved using incremental polynomial or secant methods. These methods are described in ASTME647 [17]. Due to the sectioned of the fatigue lifetime curves and data fitting, the smoothing procedure generate the similar mean values with better fitting. This effect has been demonstrated in Fig. 6b, where the exemplary FCGR curves for the specimen P1_30 are shown. The equivalent stress intensity factor has been obtained using Tanaka [18] proposal for I+II mixed loading:

$$\Delta K_{eq} = \sqrt[4]{\Delta K_I^{\ 4} + 8\Delta K_{II}^{\ 4}}. \tag{8}$$

Table 1. Summary of test results.

Specimen ID	crack initiation angle – exp.	FEM simulations	crack initiation angle – MTS [10]	crack initiation angle – SED [11-12]	Mixity parameter M_e [-]	C_e	m_e	R^2	Total lifetime/ Additional comments
30 P1	44.2°	25°	27.4°	25.4°	0.818	2e-13	6.33	0.96	374090
30 P2	54.65°	25°	27.4°	25.4°	0.816	2e-11	4.63	0.93	368047
30N1	45.8°	25°	27.4°	25.4°	0.821	7e-13	6.14	0.93	340330
30N2	49.7°	25°	27.4°	25.4°	0.818	3e-11	4.64	0.91	289089
45P1	68°	38°	33.4°	32.4°	n/a	n/a	n/a	n/a	n/a - overloaded
45P2	69.5°	38°	33.4°	32.4°	0.700	2e-8	2.35	0.94	465000
45N1	58.8°	38°	33.4°	32.4°	0.699	5e-9	2.81	0.93	740800
45N2	59.7°	38°	33.4°	32.4°	0.700	1e-8	2.54	0.76	584000
Mode I – based on [13]	0°	0°	0°	0°	1	7e-15	7.01	0.83	n/a

According to the experimental data, the crack initiation angle (θ), equivalent C_e constants and exponent m_e from the Paris' law equation were collected in Tab. 1. A noticeable fact is that the fatigue lifetime increases with the increasing of the loading angle (α). There are no sufficient statistical data for the discussion about the differences in post-operated state and normalized one. Of course, the microstructure can plays an important factor in FCGR curve description and crack paths. In almost all cases, the initiation angle was lower in group of the specimen after heat treatment. However, the most significant and valuable information from the experimental data is that for all specimens the initiation angle obtained from experiments is about two times higher than prediction from most widely used criteria. It means that for puddle iron all of the mentioned criteria are not suitable for the prediction of the fatigue crack initiation angle. The higher value of angle can be direct connected with the nonmetallic inclusions pattern (random and individual for each puddle iron). A repeatability of the crack initiation angle in each group of the specimen is verified. It confirms the need of the incorporation of an important parameter responsible for the heterogeneity-anisotropy of the material. In another work [19] it has been demonstrated that the critical values of J, $J_{0.2}$ integral, in LT direction was also much more higher than in TL direction: $J_{0.2}$(LT)=85.9 N/mm, $J_{0.2}$(TL)=29.5 N/mm. It indicates that the mixed mode loading fracture mechanics consideration is essential in understanding the brittle nature of the puddle iron in existing steel structures.

3.3. Fatigue crack paths

In Fig. 7 is shown the initial stage (approx. 1.8 mm) of the fatigue crack paths under mixed mode loading condition. As it was expected, the fatigue crack paths has been shaped by numerous of nonmetallic inclusions. Under some circumstances, the “zig-zag” type crack paths is observed and are due to the decreasing of the cohesion surface between ferrite grains and brittle nonmetallic inclusions. A good example of this type of fracture is shown in Fig. 7b. In general view, the crack path can be globally considered as a straight line – it was also confirmed by the high values of the R2 fitting crack tip coordinates measured in each 10000 cycles. A noticeable observation is the crack branching and fast propagation in ferrite grains. This phenomenon is also supported by the microstructural degradation processes – brittle precipitations allow for easy crack propagation inside ferrite grains. Finally, it can leads to the partially separations of the metal (Fig. 7 d-f).

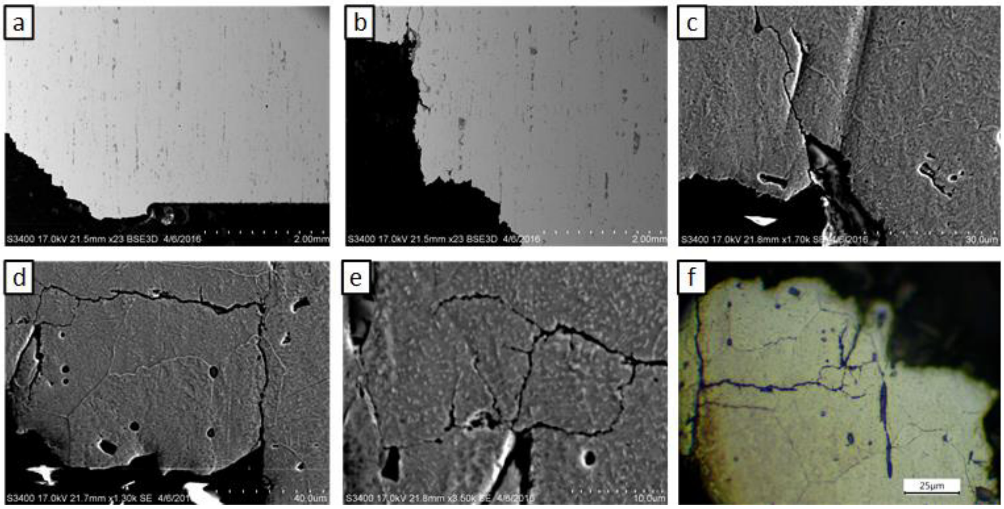

Fig. 7. Fatigue crack path in specimen P1_30; (a) mechanical notch with fatigue crack (mode I, precrack) and mixed mode crack path, SEM-BSE technique; (b) “zig-zag” type of fatigue crack path caused by the nonmetallic inclusion, SEM-BSE technique; (c) enlarged area of the remaining nonmetallic inclusion with initiated fatigue crack in ferrite grains, SEM; (d) crack branching and secondary crack propagation in ferrite grains, SEM; (e) enlarged branched fatigue crack in ferrite grain with brittle precipitations, SEM; (f) a view on the region from image (d) using light microscopy, all specimen surfaces were etched 3%HNO_3.

4. Summary and conclusions

In this paper a mixed mode fatigue fracture testing methodology has been presented. The FEM model and the experimental technique allow to obtain the kinetic fatigue fracture diagrams and crack initiation angle under mixed mode loading conditions. A long term operated puddle iron member has been devoted to this investigation. The CTS specimen and two levels of mixity (for 30° and 45° load angle) were considered. The obtained results have shown the inadequacy of the classical mixed mode fracture theories for the prediction of the crack initiation angle. The mentioned criterion are suitable for homogenous elasto-plastic metals. However, the puddle iron shows tendency to the brittleness in TL direction. It seems that for puddle iron a new criterion of the mixed mode loading should be formulated. It is also needed more experimental data, especially close to the pure shear state. However, it seems that the equivalent stress intensity factor concept can be helpful in description of the FCGR diagram. It is noticeable that for the 30° load angle, the experimental data are close to the mode I. The decreasing of the FCGR and increasing of the lifetime for the specimen loaded with higher value of load angle has been confirmed. On the other hand, the obtained values are much greater than values for modern low-carbon steel. It is also an additional hazard factor in operating of the old puddle iron structures. From the maintenance of the old structures point of view, the obtained results are valuable due to the discovered cracks in rivet hot-spot areas loaded in mixed mode manner.

Acknowledgements

This work has been supported by the Wroclaw University of Science and Technology project no 0402/0112/16(K1010). Doctor J. Correia acknowledges the Portuguese Science Foundation (FCT) for the financial support through the post-doctoral grant SFRH/BPD/107825/2015. Authors gratefully acknowledge the funding of SciTech - Science and Technology for Competitive and Sustainable Industries (NORTE-01-0145-FEDER-000022).

References

[1] De Jesus, A.M.P., et al., (2011). Strain-life and crack propagation fatigue data from several Portuguese old metallic riveted bridges. Engineering Failure Analysis, 18.1: 148-163.
[2] Lesiuk, G., Szata, M., Bocian, M., (2015). The mechanical properties and the microstructural degradation effect in an old low carbon steels after 100-years operating time, Archives of Civil and Mechanical Engineering, V 15, N 4, P 786-797.
[3] Madaj A., Wołowicki W., Construction and maintenance of bridges (in Polish), WKiŁ, Warszawa 2009
[4] Suresh, Fatigue of Materials, Cambridge University Press, Cambridge (UK), Second edition, 1998.
[5] R. Helmerich, B. Kühn, A. Nussbaumer. Assessment of existing steel structures. A guideline for estimation of the remaining fatigue life. Structure and Infrastructure Engineering, 3(3):245–255, September 2007.
[6] T. Larsson. Fatigue assessment of riveted bridges. PhD Thesis, LuleåUniversity of Technology, Department of Civil and Environmental Engineering, Division of Structural Engineering, Sweden 2009.
[7] R. Helmerich. Alte Stähle und Stahlkonstruktionen. Materialuntersuchungen, Ermüdungsversuche an orginalen Brükenträgern und Messungen von 1990 bis 2003, Bundesanstalt für Materialforschung und Prüfung (BAM), 2005
[8] Kühn B., Lukić M., Nussbaumer A., Günther H.-P., Helmerich R., Herion S., Kolstein M.H., Walbridge S., Androic B., Dijsktra O., Bucak O., Assessment of Existing Steel Structures: Recommendations for Estimation of Remaining Fatigue Life, Joint Report Prepared under the JRC – ECCS cooperation agreement for the evolution of Eurocode 3 (programme of CEN / TC 250), 2008
[9] Hellen, T.K., Blackburn, W. S. (1975). The calculation of stress intensity factors for combined tensile and shear loading. Int. J. of Fracture 11, 605-617.
[10] Erdogan, F. and Sih, G. C., On the crack extension in plates under plane loading and transverse shear. J. bas. Engng, ASME Trans., 1963, 85, 519-525.
[11] Sih, G. C., Mechanics of Fracture Initiation and Propagation. Kluwer, The Netherlands, 1991.
[12] Sih, G. C., Discussion on "Some observations on Sih's strain energy density approach for fracture prediction". Int. J. Fracture, 1974, 10, 279-284.
[13] Lesiuk G., José A.F.O. Correia, A.M.P. De Jesus, Paweł Kucharski, Fatigue crack propagation behavior of old puddle iron including crack closure effects, Procedia Structural Integrity, Volume 2, 2016, Pages 3218-3225, ISSN 2452-3216,
[14] Richard, H.A., "Bruchvorhersagen bei überlagerter normal- und schubbeanspruchung von Rissen", (in German), VDI Forschungsheft 631, VDI-Verlag, Düsseldorf, pp. 1-60, 1985.
[15] Borrego L.P, Antunes F.V, Costa J.M, Ferreira J.M. "Mixed-mode fatigue crack growth behaviour in aluminium alloy" International Journal of Fatigue, May–June 2006.
[16] Zafošnik B.; Ren Z.; Ulbin M.; and Flašker J.; "Evaluation of stress intensity factors using finite elements",FENET technology workshop, Trieste 2002
[17] ASTME647-15, Standard test methods for fatigue crack growth rate, ASTM
[18] Tanaka K,Eng.Fract.Mech.6(1974)493–507.
[19] Lesiuk G., Kucharski P., Initiation of the fracture in long-term operated steel in terms of the energy approach, TTS , Technika Transportu Szynowego, 2015, R22, 12, pp. 920-927 (in Polish).